Chemical Cleavage of Fucoxanthin from *Undaria pinnatifida* and Formation of Apo-fucoxanthinones and Apo-fucoxanthinals Identified Using LC-DAD-AP-CI-MS/MS

Junxiang Zhu, Xiaowen Sun, Xiaoli Chen, Shuhui Wang, Dongfeng Wang

PII: S0308-8146(16)30744-0
DOI: http://dx.doi.org/10.1016/j.foodchem.2016.05.064
Reference: FOCH 19213

To appear in: *Food Chemistry*

Received Date: 11 September 2015
Revised Date: 5 May 2016
Accepted Date: 11 May 2016

Please cite this article as: Zhu, J., Sun, X., Chen, X., Wang, S., Wang, D., Chemical Cleavage of Fucoxanthin from *Undaria pinnatifida* and Formation of Apo-fucoxanthinones and Apo-fucoxanthinals Identified Using LC-DAD-APCI-MS/MS, *Food Chemistry* (2016), doi: http://dx.doi.org/10.1016/j.foodchem.2016.05.064

Chemical Cleavage of Fucoxanthin from *Undaria pinnatifida* and Formation of Apo-fucoxanthinones and Apo-fucoxanthinals Identified Using LC-DAD-APCI-MS/MS

Junxiang Zhu[1], Xiaowen Sun[1], Xiaoli Chen[1], Shuhui Wang[2], Dongfeng Wang[1]*

[1] College of Food Science and Engineering, Ocean University of China, Qingdao 266003, the People's Republic of China

[2] Qingdao Municipal Center for Disease Control & Prevention, Qingdao 266033, the People's Republic of China

* Corresponding author. Tel.: +86 0532 82031575; fax: +86 0532 82032468; E-mail: wangdf@ouc.edu.cn

Acknowledgments

This work was supported by the contribution of the Specialized Research Fund for the Doctoral Program of Higher Education (Grant No. 20110132110007); the National Natural Science Foundation of China (Grant No. 31371731); and the Independent Innovation Major Project of Huangdao District Qingdao City (Grant No. 2014-3-11). We acknowledge the Drs. Xu, Fan, and Cong for their technical assistance.

Abstract: As the most abundant carotenoid in nature, fucoxanthin is susceptible to oxidation under some conditions, forming cleavage products that possibly exhibit both positive and negative health effects *in vitro* and *in vivo*. Thus, to produce relatively high amounts of cleavage products, chemical oxidation of fucoxanthin was performed. Kinetic models for oxidation were probed and reaction products were identified. The results indicated that both potassium permanganate ($KMnO_4$) and hypochlorous acid/hypochlorite ($HClO/ClO^-$) treatment fitted a first-order kinetic model, while oxidation promoted by hydroxyl radical ($OH^·$) followed second-order kinetics. With the help of liquid chromatography-tandem mass spectrometry, a total of 14 apo-fucoxanthins were detected as predominant cleavage products, with structural and geometric isomers identified among them. Three apo-fucoxanthinones and eleven apo-fucoxanthinals, of which five were *cis*-apo-fucoxanthinals, were detected upon oxidation by the three oxidizing agents ($KMnO_4$, $HClO/ClO^-$, and $OH^·$).

Keywords: fucoxanthin, apo-fucoxanthins, chemical cleavage, reaction kinetics, LC-DAD-APCI-MS/MS

Chemical compounds studied in this article

Fucoxanthin (PubChem CID: 5281239)

1. Introduction

Fucoxanthin is the principal carotenoid present in the chloroplasts of brown seaweed. It is the most abundant of all carotenoids, accounting for more than 10% of their estimated total natural production (Miyashita et al., 2011). Numerous beneficial nutritional and medicinal properties of fucoxanthin have been reported, including excellent antioxidant (Fung, Hamid, & Lu, 2013; Takashima, Shichiri, Hagihara, Yoshida, & Niki, 2012), anti-cancer (Satomi, 2012; Ye et al., 2014), anti-obesity (Maeda, Hosokawa, Sashima, Funayama, & Miyashita, 2005; Kang et al., 2012), anti-inflammatory (Heo et al., 2010) and anti-angiogenic (Sugawara, Matsubara, Akagi, Mori, & Hirata, 2006) activity. Furthermore, fucoxanthin can help prevent bone diseases, such as osteoporosis and rheumatoid arthritis (Das, Ren, Hashimoto, & Kanazawa, 2010). These findings indicate that fucoxanthin can be used as a nutritional supplement in diet or functional food, with a potential to lower the incidence of obesity, cardiovascular disease, diabetes and cancer.

The distinct structure of fucoxanthin includes an unusual allenic bond, epoxy group, and conjugated double bond in the polyene chain (Fig. 1). This structure is highly unstable under some external conditions. In the previous study (Zhao, Kim, Pan, & Chung, 2014), the decrease of total fucoxanthin and increase of *cis*-fucoxanthins, owing to thermal processing, air exposure, and illumination, can be observed in canola oil. Besides the isomerization, carotenoids are also susceptible to oxidation, generating a great diversity of short-chain carbonyl compounds and, in some cases, some volatile compounds (de Jesus Benevides, da Cunha Veloso, de Paula Pereira, &

de Andrade, 2011). However, these compounds are not investigated in the relatively few fucoxanthin stability studies (Kawee-ai, Kuntiya, & Kim, 2013; Sugimura et al., 2012; Zhao, Kim, Pan, & Chung, 2014).

Besides the color fading, the products of carotenoid degradation are also supposed to exhibit both positive and negative effects *in vitro* and *in vivo*. Taking lutein as an example, its breakdown products have been reported to induce cytotoxic and genotoxic effects in human retinal pigment epithelial cells (Kalariya, Ramana, Srivastava, & van Kuijk, 2008; Kalariya, Ramana, Srivastava, & van Kuijk, 2009). However, Nidhi, Sharavana, Ramaprasad and Vallikannan (2015) appraised the anti-inflammatory efficacy of lutein UV-mediated cleavage products in counteracting inflammation caused by lipopolysaccharide in rats. The results suggested that lutein oxidation/photolysis produced fragments that exhibited higher antioxidant and anti-inflammatory effects than the parent lutein molecule. Thus, an in-depth understanding of carotenoid oxidative cleavage is significant not only for avoiding the deterioration of fucoxanthin-enriched food quality during processing and storage, but also for predicting possible effects on human health.

Normally, a trace amount of degradation products is formed in a complex food matrix, which makes their detection and identification difficult (Rodriguez, & Rodriguez-Amaya, 2009). So in some previous studies, carotenoid cleavage was performed with chemical methods to produce relatively high amounts of derivatives with explicit structure (Caris-Veyrat, Schmid, Carail, & Böhm, 2003; Pennathur et al., 2010; Sy, Dangles, Borel, & Caris-Veyrat, 2013). In addition, chemical oxidation can

be used to investigate the stability of carotenoids under simulated food processing conditions. For instance, de Jesus Benevides, da Cunha Veloso, de Paula Pereira and de Andrade (2011) studied the ozonolysis of β-carotene, where solutions of this compound were exposed to ozone concentrations similar to those used in the food sanitization process.

Therefore, this work is dedicated to the investigation of chemical ($KMnO_4$, $HClO/ClO^-$ and $OH^·$) oxidation of fucoxanthin, probing the corresponding kinetic models and identifying cleavage products, which could possibly underpin a further study on bioactivity and safety evaluation of these products *in vivo*.

2. Materials and methods

2.1. Materials and Chemicals

Dried seaweed (*Undaria pinnatifida*) was purchased from Rongcheng Jiayi Aquatic Food Co., Ltd., Weihai, China. All dried samples were pulverized using a micro plant grinder and sieved (200 μm sieves) to obtain a fine powder. The dried seaweed powders were stored in the dark at room temperature until used.

The standard of all-*trans* fucoxanthin was acquired from Sigma Chemical Company (St. Louis, MO, USA). Solvents for HPLC including acetonitrile and methyl *tert*-butyl ether (MTBE) were provided by Merck (Darmstadt, Germany). $KMnO_4$, iron(II) chloride tetrahydrate ($FeCl_2·4H_2O$), hydrogen peroxide (H_2O_2), sodium hypochlorite (NaClO) and hydrochloric acid (HCl) were supplied by Sinopharm Chemical Reagent Co., Ltd. (Shanghai, China). All other reagents used were of analytical grade.

2.2. Isolation of fucoxanthin from Undaria pinnatifida

The extraction process was conducted using the methodology described by Xia et al. (2013) with some modifications. All extractions were carried out in the dark to reduce the possibility of photo-oxidation. Appropriate amounts of seaweed powders were mixed with 80% (v/v) ethanol containing 0.01% (w/v) butylated hydroxytoluene (BHT) to obtain a concentration of 0.25 g/mL. The mixtures were initially stirred by an overhead stirrer for 0.5 h at room temperature, followed by static extraction, which was conducted at 40 °C for 11.5 h and repeated three times. The extracts were centrifuged at 5000 × *g* for 15 min and concentrated *in vacuo*. 95% (v/v) methanol/hexane (1:1, v/v) was added to the ethanolic extract to isolate fucoxanthin. After stirring for 1 min, mixtures separated into two distinct layers in a separation funnel. The upper phase was discarded, and the lower one was concentrated for use in subsequent experiments.

According to the modified methodology of fucoxanthin purification described by Maeda, Hosokawa, Sashima, Funayama and Miyashita (2005), methanolic extracts were subjected to silica gel adsorption chromatography. Silica gel (200-300 meshes, Qingdao, China) was slurry-packed into a glass column and equilibrated with petroleum ether/ethyl acetate (1:1, v/v). Extracts were adsorbed by portions of silica gel of the same weight, loaded on the top of the column, and eluted in the dark using a linear gradient of petroleum ether/ethyl acetate from 1:1 to 1:9 (v/v) for 60 min. Fractions with different colors, i.e., green, reddish-orange, chartreuse, emerald and yellow (from the top down), were collected in test tubes for HPLC analysis.

2.3. HPLC-VWD analysis

To determine whether the fractions collected during the purification process contained fucoxanthin, each portion eluted from the column was analyzed by an HPLC system (1100, Agilent Technologies Inc., Santa Clara, CA, USA) equipped with an autosampler, a column oven, and a variable wavelength detector (VWD). A ZORBAX SB-C18 column (4.6 × 250 mm, 5 μm, Agilent Technologies Inc., Palo Alto, CA, USA) was used at 25 °C, with the detection wavelength was set to 450 nm. A gradient system based on a slight modification of a previous study (Zhao, Kim, Pan, & Chung, 2014) was used. Elution was performed at a flow rate of 0.8 mL/min with linear gradients of solvents A and B (A: acetonitrile/water 80/20, v/v; B: MTBE). The solvent gradient used was 100% A at the start, with B linearly increased from 0 to 10% in 10 min and held constant for 10 min before returning to initial conditions in 5 min. At the end of the run, the system was equilibrated with 100% solvent A for 7 min. After HPLC analysis, the fractions containing fucoxanthin were collected and concentrated to a small volume, dried under nitrogen, and then stored in ethanol at –20 °C until used.

2.4. Chemical oxidation procedure

Modified oxidation methodologies from previous studies (Gurak, Mercadante, González-Miret, Heredia, & Meléndez-Martínez, 2014; Sommerburg et al., 2003; Woodall, Lee, Weesie, Jackson, & Britton, 1997) utilizing $KMnO_4$, $HClO/ClO^-$, and $OH^·$ were used, and the optical spectra were recorded on a Unico UV2102-PC UV-visible spectrophotometer (Shanghai, China). The prepared fucoxanthin diluted with dichloromethane (1.5 mL, 0.13 mM) was treated with 1 mL of 0.8 mM $KMnO_4$,

1 mL of 2.3 M NaClO containing 0.1 mL HCl (1 M), or 1 mL of 9.9 M H_2O_2 containing 0.2 mL $FeCl_2$ solution (10 mM). The reaction mixtures were continuously vortexed (4-32 min) in the dark, then washed five times using distilled water. After centrifuging at 7000 × *g* for 2 min, the organic layer was separated under a steam of nitrogen and re-dissolved in 1.5 mL dichloromethane for spectral analysis. The UV-vis spectra were recorded from 200 to 700 nm, with the absorbance at 449 nm used as a measure of fucoxanthin concentration in the following rate equation:

$$\frac{dA}{dt} = -kA^n \quad (1)$$

Here *A*, *t*, *k* and *n* represent the absorbance at 449 nm, the reaction time (min), the reaction rate constant (min^{-1}) and the kinetic order of the reaction, respectively. Equation 1 can be integrated to obtain concentration as a function of time. For a degradation reaction, integration of Equation 1 for *n* = 0, 1 and 2 (for zero-, first- and second-order kinetics) leads to Equations 2, 3 and 4, which have been widely used to model quality changes in carotenoid-rich foods owing to its simplicity and satisfactory fit to experimental data (Van Boekel, 2008):

$$A = A_0 - kt \quad (2)$$

$$A = A_0 e^{-kt} \quad (3)$$

$$A = \frac{A_0}{1 + kA_0 t} \quad (4)$$

Where, A_0 is the initial absorbance of fucoxanthin at 449 nm. The best fit was determined based on the respective coefficients of determination (R^2), and the kinetic parameters were estimated by non-linear regression using Origin 8 (Microcal Origin,

USA).

2.5. LC-DAD-APCI-MS/MS analysis

The oxidation and control groups were analyzed using an HPLC system (1260, Agilent Technologies Inc., USA) equipped with an autosampler, a column oven, a diode array detector (DAD) and a triple quadrupole mass spectrometer with atmospheric pressure chemical ionization (APCI) interface operated in positive ionization mode. Samples were injected onto a ZORBAX Eclipse XDB-C18 column (4.6 × 250 mm, 5 μm, Agilent Technologies Inc., USA). The mobile phase used a gradient of solvent A (acetonitrile/water 80/20, v/v) and B (acetonitrile/water/MTBE 68/17/15, v/v/v). The flow was maintained at 0.8 mL/min, and the sample injection volume was 10 μL. Detection wavelengths for UV-vis were set at 300, 350, and 400 nm. The following gradient flow program was used: mobile phase B increased from 0 to 60% in 10 min and kept constant for 10 min, then changed back to 0% in 7 min. The MS operation parameters were adapted from Pennathur et al. (2010): capillary voltage 2500 V, drying gas flow 5 L/min, drying gas temperature 350 °C, vaporizer temperature 450 °C, and nebulizer pressure 20 psi. The mass range between *m*/*z* 200 and 800 was used for full scan mass spectra. The optimal fragmentor voltage for fucoxanthin was 10 V, with a mass range of *m*/*z* 100 to 700 for MS/MS scan modes containing product and precursor ion scans. The Agilent MassHunter (version 3.1) software package was used for data acquisition and analysis (Agilent Technologies Inc., USA).

3. Results and discussion

191 *3.1. Preparation of unoxidized fucoxanthin from Undaria pinnatifida*

192 The fucoxanthin used in the chemical oxidation procedure was initially isolated from
193 *Undaria pinnatifida* by conventional solvent extraction, and the various purified
194 fractions were collected after silica gel column chromatography. The results of HPLC
195 analysis indicated the presence of fucoxanthin in both the crude extracts and the
196 reddish-orange pigment fraction. As shown in Fig. S1, peak I with a retention time of
197 11.48 min corresponded to the all-*trans* fucoxanthin as compared with the standard.
198 Similarly, previous research on color profiles of carotenoids separated by thin-layer
199 chromatography illustrated that fucoxanthin was a characteristic orange pigment
200 present in *Undaria pinnatifida* and *Ectocarpus siliculosus* (Mikami, & Hosokawa,
201 2013). In the LC-DAD-APCI-MS spectrum of the purified sample (Fig. S2), peak I
202 with a retention time of 12.49 min and a characteristic spectral signal of all-*trans*
203 fucoxanthin (λ_{max}: 449 and 466 nm) was detected, with a relative content of up to
204 84.39%. Moreover, peaks II, III and IV with respective relative contents of 0.60%,
205 2.83% and 12.18% were identified as three *cis*-fucoxanthin isomers based on their
206 UV-vis spectra (Fig. S2B) and mass-spectrometric behavior (Fig. S2C). In the latter
207 analysis, the base peak in the full MS of all three isomers corresponded to dehydrated
208 protonated analyte with *m*/*z* 641. Specifically, compounds eluted at 13.16, 16.57, and
209 18.27 min were identified as 13,13'-*cis*-, 9'-*cis*-, and 13'-*cis*-fucoxanthin respectively,
210 in line with their hypsochromic shift peculiarity and the intensity of the *cis* peak
211 (DB/DII: 23.8, 10.2, 47.5%) according to prior research of Haugan, Englert, Glinz
212 and Liaacn-Jensen (1992). Since almost no other peaks were present in the

chromatogram of the isolates from *Undaria pinnatifida*, the purified seaweed extracts could be used as an unoxidized fucoxanthin sample for subsequent experiments.

3.2. Spectrum and kinetic analysis of fucoxanthin oxidation

Chemical oxidants, including $KMnO_4$, $HClO/ClO^-$ and $OH^·$ are versatile reagents that can react with carbon-carbon double bonds in carotenoids via diverse mechanisms to produce different types of products. As a result of chemical oxidation, the pigment in the model system faded, while its absorption peak flattened, shifted and finally disappeared (Figs. 2A–2C). The spectral changes observed for the three reactions indicated that the generated products were similar, based on the shift of λ_{max} values from 400–500 nm to 300–400 nm after oxidation for 30 min. The structure of fucoxanthin features an unsaturated chain with seven conjugated double bonds, and its characteristic UV-visible spectra exhibit a hyperconjugative effect (Fig. 1). The disappearance of the fucoxanthin signal could be attributed to hyperconjugation loss after oxidation (Pennathur et al., 2010). Furthermore, the kinetics of fucoxanthin color loss in the reaction with chemical oxidants was investigated. After 30 min of oxidation using $KMnO_4$ and $HClO/ClO^-$, a 60 and 87% decrease of fucoxanthin concentration was observed (Fig. 2D), respectively. Similarly, when fucoxanthin was oxidized by $OH^·$, increasing the reaction time from 0 to 32 min caused a continued reduction (0 to 77%) of absorption at 449 nm. The respective R^2 of 0.976 and 0.990 indicated that both $KMnO_4$ and $HClO/ClO^-$ showed a good fit to a first-order kinetic model (n = 1), with the rate constants of 3.12×10^{-2} and 7.65×10^{-2} min^{-1}, respectively. Nevertheless, the reaction with $OH^·$ followed the second-order kinetics

(R^2 = 0.966, n = 2), with $k = 1.69 \times 10^{-1}$ min^{-1}. The observed difference illustrated that the mechanism of fucoxanthin with $KMnO_4$ and $HClO/ClO^-$ was different to that with $OH^{\cdot}$. Variation of kinetic order may be attributed to the complexity of carotenoid behavior in radical-scavenging reactions, which includes the formation of carotenoid/hydroxyl adducts and carotenoids radicals ($Car^{\cdot}$). In the field of non-thermal food processing, the second-order kinetic model was used to describe ultrasonic degradation of β-carotene in dichloromethane (Sun, Ma, Ye, Kakuda, & Meng, 2010), which was also related to the reaction between carotenoids and free radicals produced by ultrasound (Riesz, Berdahl, & Christman, 1985).

3.3. MS scan of fucoxanthin cleavage products

LC-MS technology has exerted a huge effect on the analysis of carotenoids, including structure elucidation premised on molecular mass and fragmentation pattern. APCI has become the most commonly used ionization technique for carotenoids, showing high analytical sensitivity and being suitable for the ionization of carotenoids with different polarities (Rivera, & Canela-Garayoa, 2012). Thus, LC-APCI-MS was utilized to determine whether the observed reaction products were indeed due to the oxidation and fragmentation of the parent fucoxanthin molecule.

The maximum absorbance of carotenoid cleavage products is dependent on the number of conjugated double bonds present (Weesepoel, Gruppen, de Bruijn, & Vincken, 2014). To detect the widest possible array of oxidation products using DAD, detection wavelengths were set at 300, 350 and 400 nm based on the results of spectral analysis (Figs. 2A–2C). Using these three wavelengths, a plethora of peaks

generated by $KMnO_4$-accelerated oxidation were detected, of which 17 could be tentatively assigned (Fig. S3A). Some previous studies on carotenoid oxidation with potassium permanganate (Caris-Veyrat, Schmid, Carail, & Böhm, 2003; Rodriguez, & Rodriguez-Amaya, 2009; Gurak, Mercadante, González-Miret, Heredia, & Meléndez-Martínez, 2014) indicated that oxygenated products found in the reaction mixtures were apo-carotenoids. For example, potassium permanganate used by Rodriguez and Rodriguez-Amaya (2009) could cleave the double bonds of lycopene and generate apo-lycopenals without further oxidation to carboxylic acid. In this reaction, a [3+2] electrocyclic addition of permanganate ion to the π-bond may be a part of the initial step, leading to the formation of a cyclic Mn(V) ester. Intramolecular electron transfer subsequently occurs to give the oxidized cyclic Mn(VI) ester, which, in turn, produces final products bearing aldehyde groups by rearrangement and fragmentation (Fatiadi, 1987).

Compared with the $KMnO_4$-accelerated oxidation, the reaction with $HClO/ClO^-$ produced similar products based on the resemblance of two chromatogram profiles. As shown in Fig. S3B, 19 peaks found using different detection wavelengths and eluted approximately between 2 and 8 min could be tentatively assigned. These oxidation products were likewise identified as apo-carotenoids in a previous study on astaxanthin (Weesepoel, Gruppen, de Bruijn, & Vincken, 2014). In this reaction, the electron-rich olefin moiety in fucoxanthin initially acts as a nucleophile, with the chloride atom of $HClO/ClO^-$ acting as an electrophile. After the formation of a transformable carbonium ion, followed by the opening of the chloronium ion ring and

an intramolecular S_N2-type reaction of the formed chlorohydrin, fucoxanthin epoxides are formed. When the epoxides encounter a second HClO molecule, the cleavage of the carbon-carbon bond proceeds to generate two aldehydes (Pennathur et al., 2010). When compared with the reactions of $KMnO_4$ and $HClO/ClO^-$, the retention time of various peaks observed in the $OH^·$-promoted oxidation was also in the range from 2 to 8 min, as shown in Fig. S3C. Scavenging of $OH^·$ generated in the Fenton reaction had been investigated in the studies of carotenoids *in vitro* antioxidant activity. Fucoxanthin and its stereoisomers were chosen as targets for the evaluation of their $OH^·$ scavenging activity using chemiluminescence and electron spin-resonance spectroscopy (D'Orazio et al., 2012; Zhang et al., 2014). When it comes to carotenoid-radical interaction, the primary products of hydrogen abstraction from carotenoids by $OH^·$ are the corresponding radicals ($Car^·$), with the final degradation products frequently being carbonyls and epoxides (Krinsky, & Yeum, 2003). One of the reasons for their formation is the generation of carotenoids oxy-radicals ($Car–O^·$), comparable to the alkoxyl radicals ($LO^·$) produced during lipid peroxidation, leading to the cleavage of the polyene chain. A conceivable reaction sequence to generate the $Car–O^·$ is as follows: $Car + OH^· \rightarrow Car^· + H_2O$; $Car^· + O_2 \rightarrow Car–OO^·$; $Car–OO^· + Car \rightarrow Car–OOH + Car^·$; $Car–OOH + Fe^{2+} \rightarrow Car–O^· + Fe^{3+} + OH^-$. The $Car–O^·$ radical is more reactive than either $Car^·$ or carotenoid peroxy radicals ($Car–OO^·$) and is able to abstract an electron from adjacent carbon-carbon bonds to form two products. The latter reaction is known as β-scission. Additionally, $Car–O^·$ can also lose an electron to become a ketone, or bond to an adjacent carbon to

form an epoxide (Damodaran, Parkin, & Fennema, 2007).

In view of the above-mentioned studies, oxidation products obtained with the three chemicals listed above were normally identified as apo- and epoxy-carotenoids. Therefore, ion chromatograms of various degradation compounds with different predicted *m/z*, including apo- and epoxy-fucoxanthins, were extracted from the total ion chromatograms (TICs) of the mass spectra. The retention time in respective extracted ion chromatograms (EICs) was compared with the values shown in Fig. S3. Similarly to preceding research, the results showed the presence of apo-fucoxanthinals and apo-fucoxanthinones, whereas apo-fucoxanthinoic acids and epoxy-fucoxanthins were not detected in the reactions of fucoxanthin with $KMnO_4$, $HClO/ClO^-$ and OH^- in this study. Some predominant fucoxanthin cleavage products with *m/z* 267, 293, 307, 333, 359, 399, and 425 had different retention time in the APCI positive mode. Although only oxidative modification was applied, the compounds with *m/z* 267, 333, 359, and 425 were difficult to identify, since they can exhibit structural or configurational isomerism, which was the main distinction between fucoxanthin and other common carotenoids upon oxidative cleavage of the polyene chain.

3.4. MS/MS fragments of fucoxanthin cleavage products

Since most carotenoids showed little fragmentation during APCI mass spectrometry, collision-induced dissociation with product ion tandem mass spectrometry could be helpful for structural characterization and elucidation of whether the observed reaction products are indeed attributable to oxidation (van Breemen, Dong, &

Pajkovic, 2012). Then identification was further verified by analyzing MS/MS fragmentation of all $[M+H]^+$ parent ions assigned. To optimize the MS/MS parameters the prepared fucoxanthin was first analyzed in APCI positive ionization mode. Protonated fucoxanthin with *m/z* 659, $[M+H]^+$, was detected as the base peak corresponded to the loss of water at *m/z* 641, $[M+H-18]^+$, which is characteristic for a compound with a hydroxyl group. The molecular ion peak with second-highest relative abundance was observed at *m/z* 581 corresponding to the elimination of water and acetic acid, $[M+H-18-60]^+$, from protonated fucoxanthin (Fig. S2C). The three molecular ions, $[M+H]^+$, $[M+H-18]^+$ and $[M+H-18-60]^+$, were fragmented at various voltages. The optimal voltage to obtain maximal structural information in the MS/MS scan mode was determined to be 10 V.

Fig. S4 showed the EICs for *m/z* 293 (apo-11'-fucoxanthinal), which was located with the full scan MS data accompanying a chromatographic peak in Fig. S3. As shown in Fig. 3A, this compound fragmented to form a daughter ion with *m/z* 233, corresponding to the loss of acetic acid, $[M+H-60]^+$, which further ascertained the structure of apo-11'-fucoxanthinal. Another fragment ion of *m/z* 125, $[M+H-18-56-94]^+$, was produced from the protonated molecule by cleavage the C6'–C7' bond of the polyene chain, with a loss of 56 amu previously observed in APCI mass spectra of carotenoids containing an ε-ring (Rivera, Christou, & Canela-Garayoa, 2014).

A product with *m/z* 307 was detected in the oxidation reactions with $HClO/ClO^-$ and OH^-, but not with $KMnO_4$. Similarly to apo-11'-fucoxanthinal, it was situated with the

full scan MS data accompanying only a chromatographic peak labeled as 2 in Figs. S3B and S3C. As shown in Fig. 3B, an ion with *m/z* 289, $[M+H-18]^+$, and its derivative at *m/z* 207, $[M+H-18-82]^+$, were observed, which indicated that the dehydrated molecule underwent further bond cleavage between C9 and C10. Another ion with *m/z* 109 was detected, attributable to bond cleavage between carbons 6, 7 and 12, 13.

As mentioned earlier, two structures were plausible for the compound at *m/z* 267: apo-11-fucoxanthinal and apo-9'-fucoxanthinone. However, when comparing its EIC (Fig. S4) with the chromatograms (Fig. S3), it located with the full scan MS data was accompanied by only one chromatographic peak, denoted as 16, 18 and 19 in Figs. S3A, S3B and S3C, respectively. MS/MS spectra were helpful for the structural characterization. As shown in Fig. 3C, the fragmentation of peak 16 in Fig. S3A was explained by consecutive cleavage of the end ring and the double bond between C7' and C8', yielding two fragment ions with *m/z* 211 ($[M+H-56]^+$) and *m/z* 155 ($[M+H-56-56]^+$), which suggested that the structure of the compound with *m/z* 267 corresponded to apo-9'-fucoxanthinone rather than to apo-11-fucoxanthinal.

Analogous to apo-9'-fucoxanthinone (*m/z* 267), fragmentation patterns of the two possible structural isomers of *m/z* 333 were studied using tandem mass spectrometry to facilitate the distinction. To be exact, isomers with *m/z* 333 could have either apo-15-fucoxanthinal or apo-13'-fucoxanthinone structures. When scrutinizing the chromatograms and EICs in the MS scan mode, the compounds with *m/z* 333 were found to take up two chromatographic peaks (Fig. S3). When fucoxanthin was

subjected to $KMnO_4$-promoted oxidation, one isomer of *m*/*z* 333 with a retention time of 3.307 min was identified as apo-13'-fucoxanthinone based on the presence of two fragment ions of *m*/*z* 135 and 161, as presented in Fig. 4A. The former was generated from the protonated molecule by bond cleavage between C6' and C7' carbons of the polyene chain, and the latter was produced by cleaving the double bond between C11' and C12', combined with the elimination of acetic acid and fragmentation of the end ring. Another isomer of *m*/*z* 333 eluted at 3.460 min was identified as apo-15-fucoxanthinal, showing a characteristic ion with *m*/*z* 287, produced by loss of the terminal hydroxyl and carbonyl (Fig. 4B). In addition, both isomers shared a common ion with *m*/*z* 109, ascribed to fragmentation patterns related to the various splitting sites between conjugated double bonds.

Peak 4 and 6 in Fig. S3A belonging to the compounds with *m*/*z* 359 were identified as apo-14'-fucoxanthinal and apo-15'-fucoxanthinal, respectively, based on their tandem mass spectra. As shown in Fig. 4D, an iconic ion produced from ionized compound of peak 4 was detected at *m*/*z* 205 and corresponded to the demethylated and dehydrated terminal ring with cleavage of the double bond between C10 and C11, which verified the structure of apo-14'-fucoxanthinal. Besides, the presence of the representative ion with *m*/*z* 227 (Fig. 4C), $[M+H-60-30-42]^+$, corresponding to the elimination of acetic acid and two methyl groups combined with bond rupture between C13' and C14', demonstrated that the compound of peak 6 was apo-15'-fucoxanthinal. Similarly to the mass spectrometric behavior of isomers with *m*/*z* 333, a common ion peak for apo-14'-fucoxanthinal and apo-15'-fucoxanthinal had *m*/*z* 109. Another

common ion of the two isomers was *m*/*z* 161, corresponding to carbon-carbon bond cleavage at positions 7, 8 and 14', 15' for the former, and at the 6', 7' double bond for the latter.

When matching the Fig. S4 with the Fig. S3, it could be observed that compounds with *m*/*z* 425 were ascribed to multiple chromatographic peaks, i.e., 10, 14 and 15 in Fig. S3A. Although two constitutional isomers with a relative molecular mass of 424 existed (i.e., apo-12-fucoxanthinal and apo-10'-fucoxanthinal), the MS/MS result suggested that the structure corresponded to apo-12-fucoxanthinal, due to the presence of characteristic ions with *m*/*z* 425 in all cases. As depicted in Figs. 5A–5C, the loss of toluene observed for most of the carotenoids was involved in the production of fragment ions with *m*/*z* 255. This fragmentation indicated the presence of extensive conjugation within the molecule (Rivera, Christou, & Canela-Garayoa, 2014). Additional ions were generated by cleavage of various carbon-carbon single or double bonds as discussed above. Probably, the three peaks corresponded to the different geometrical isomers of apo-12-fucoxanthinal. Since *cis*-isomers, including 13,13'-*cis*-, 9'-*cis*- and 13'-*cis*-fucoxanthin, were also formed from all-*trans*-fucoxanthin in our unoxidized samples isolated from *Undaria pinnatifida*, this conclusion seemed plausible. Based on the hypsochromic shift in λ_{max}, the *cis* absorption peak (Fig. 5D) and the elution order of *cis*-fucoxanthins, peaks 10, 14 and 15 in Fig. S3A were tentatively identified as all-*trans*-apo-12-fucoxanthinal, 9'-*cis*-apo-12-fucoxanthinal, and 13'-*cis*-apo-12-fucoxanthinal, respectively.

By the same token, *cis*-*trans* isomers were possible for *m*/*z* 399, which had only one

411 possible chemical skeleton (apo-12'-fucoxanthinal). However, they were ascribed to a
412 number of chromatographic peaks, i.e., 9, 10, 11 and 12 in Fig. S3A. When
413 fucoxanthin underwent $KMnO_4$-promoted oxidation, the generated peak 10 was
414 associated with both major and minor compounds with *m/z* 425 and *m/z* 399,
415 respectively. This bore a similarity to a previous study, which showed that the
416 chromatographic peak representing apo-12-fucoxanthinal was contaminated with
417 apo-11'-fucoxanthinal and apo-9'-fucoxanthinone, identified using mass spectrometry
418 and UV absorption spectroscopy, when fucoxanthin was allowed to react with the
419 zinc permanganate (Bonnett et al., 1969). As shown in Figs. S5A-5D, common ions
420 including *m/z* 109, 127, 173, 201, and 381 could be detected, in accordance with the
421 structure of apo-12'-fucoxanthin. Identification of *cis*-isomers with *m/z* 399 was
422 conducted similarly to above method for apo-12-fucoxanthinal isomers, although the
423 UV-vis absorbance spectrum of peak 10 was not available. Peak 9, 11 and 12 in Fig.
424 S3A with *m/z* 399 were tentatively identified as all-*trans*-apo-12'-fucoxanthinal,
425 13,13'-*cis*-apo-12'-fucoxanthinal, and 13'-*cis*-apo-12'-fucoxanthinal, respectively.
426 Finally, all apo-fucoxanthins formed during the chemically accelerated oxidation of
427 fucoxanthin were listed in Table 1.

428 **4. Conclusion**

429 Successful identification of fucoxanthin oxidation products by
430 LC-DAD-APCI-MS/MS demonstrates that a number of apo-fucoxanthinones and
431 apo-fucoxanthinals are formed in a relatively high amount when the fucoxanthin
432 isolated from *Undaria pinnatifida* is subjected to chemical cleavage using $KMnO_4$,

HClO/ClO^-, and $OH^·$. These compounds may be produced and further transformed under some food processing and stored conditions. In addition to the quantitative analysis of these products in fucoxanthin-enriched food during storage, future studies should fully investigate the nutritional health and toxicity effects of diets or functional foods with sufficient fucoxanthin content.

438 **Supplementary data**

439 Additional HPLC-VWD analysis of crude extracts and purified reddish-orange
440 fraction of *Undaria pinnatifida* in Fig. S1, LC-DAD-APCI-MS analysis of purified
441 fraction of *Undaria pinnatifida* in Fig. S2, liquid chromatograms of fucoxanthin after
442 chemical degradation in Fig. S3, EICs of apo-fucoxanthins produced by reactions of
443 fucoxanthin with $KMnO_4$, $HClO/ClO^-$, and $OH^·$ in Fig. S4, MS/MS spectra of Peak 9,
444 10, 11, 12 and UV-vis spectra of Peak 9, 11, 12 from $KMnO_4$-accelerated oxidation in
445 Fig. S5.

References

Bonnett, R., Mallams, A. K., Spark, A. A., Tee, J. L., Weedon, B. C. L., & McCormick, A. (1969). Carotenoids and related compounds. Part XX. Structure and reactions of fucoxanthin. *Journal of the Chemical Society C: Organic*, *3*, 429–454.

Caris-Veyrat, C., Schmid, A., Carail, M., & Böhm, V. (2003). Cleavage products of lycopene produced by in vitro oxidations: characterization and mechanisms of formation. *Journal of Agricultural and Food Chemistry*, *51*, 7318–7325.

Damodaran, S., Parkin, K. L., & Fennema, O. R. (Eds.). (2007). Fennema's food chemistry. CRC press.

Das, S. K., Ren, R., Hashimoto, T., & Kanazawa, K. (2010). Fucoxanthin induces apoptosis in osteoclast-like cells differentiated from RAW264. 7 cells. *Journal of Agricultural and Food Chemistry*, *58*, 6090–6095.

de Jesus Benevides, C. M., da Cunha Veloso, M. C., de Paula Pereira, P. A., & de Andrade, J. B. (2011). A chemical study of β-carotene oxidation by ozone in an organic model system and the identification of the resulting products. *Food Chemistry*, *126*, 927–934.

D'Orazio, N., Gemello, E., Gammone, M. A., de Girolamo, M., Ficoneri, C., & Riccioni, G. (2012). Fucoxantin: A treasure from the sea. *Marine Drugs*, *10*, 604–616.

Fatiadi, A. J. (1987). The classical permanganate ion: still a novel oxidant in organic chemistry. *Synthesis*, *2*, 85–127.

Fung, A., Hamid, N., & Lu, J. (2013). Fucoxanthin content and antioxidant properties of *Undaria pinnatifida*. *Food Chemistry*, *136*, 1055–1062.

Gurak, P. D., Mercadante, A. Z., González-Miret, M. L., Heredia, F. J., & Meléndez-Martínez, A. J. (2014). Changes in antioxidant capacity and colour associated with the formation of β-carotene

epoxides and oxidative cleavage derivatives. *Food Chemistry*, *147*, 160–169.

Haugan, J. A., Englert, G., Glinz, E., & Liaacn-Jensen, S. (1992). Algal carotenoids. 48.* structural assignments of geometrical. *Acta Chemica Scandinavica*, *46*, 389–395.

Heo, S. J., Yoon, W. J., Kim, K. N., Ahn, G. N., Kang, S. M., Kang, D. H., et al. (2010). Evaluation of anti-inflammatory effect of fucoxanthin isolated from brown algae in lipopolysaccharide-stimulated RAW 264.7 macrophages. *Food and Chemical Toxicology*, *48*, 2045–2051.

Kalariya, N. M., Ramana, K. V., Srivastava, S. K., & van Kuijk, F. J. (2008). Carotenoid derived aldehydes-induced oxidative stress causes apoptotic cell death in human retinal pigment epithelial cells. *Experimental Eye Research*, *86*, 70–80.

Kalariya, N. M., Ramana, K. V., Srivastava, S. K., & van Kuijk, F. J. (2009). Genotoxic effects of carotenoid breakdown products in human retinal pigment epithelial cells. *Current Eye Research*, *34*, 737–747.

Kang, S. I., Shin, H. S., Kim, H. M., Yoon, S. A., Kang, S. W., Kim, J. H., et al. (2012). *Petalonia binghamiae* extract and its constituent fucoxanthin ameliorate high-fat diet-induced obesity by activating AMP-activated protein kinase. *Journal of Agricultural and Food Chemistry*, *60*, 3389–3395.

Kawee-ai, A., Kuntiya, A., & Kim, S. M. (2013). Anticholinesterase and antioxidant activities of fucoxanthin purified from the microalga *Phaeodactylum tricornutum*. *Natural Product Communications*, *8*, 1381–1386.

Krinsky, N. I., & Yeum, K. J. (2003). Carotenoid-radical interactions. *Biochemical and Biophysical Research Communications*, *305*, 754–760.

490 Maeda, H., Hosokawa, M., Sashima, T., Funayama, K., & Miyashita, K. (2005). Fucoxanthin from
491 edible seaweed, *Undaria pinnatifida*, shows antiobesity effect through UCP1 expression in white
492 adipose tissues. *Biochemical and Biophysical Research Communications*, *332*, 392–397.
493 Mikami, K., & Hosokawa, M. (2013). Biosynthetic pathway and health benefits of fucoxanthin, an
494 algae-specific xanthophyll in brown seaweeds. *International Journal of Molecular Sciences*, *14*,
495 13763–13781.
496 Miyashita, K., Nishikawa, S., Beppu, F., Tsukui, T., Abe, M., & Hosokawa, M. (2011). The allenic
497 carotenoid fucoxanthin, a novel marine nutraceutical from brown seaweeds. *Journal of the*
498 *Science of Food and Agriculture*, *91*, 1166–1174.
499 Nidhi, B., Sharavana, G., Ramaprasad, T. R., & Vallikannan, B. (2015). Lutein derived fragments
500 exhibit higher antioxidant and anti-inflammatory properties than lutein in lipopolysaccharide
501 induced inflammation in rats. *Food & Function*, *6*, 450–460.
502 Pennathur, S., Maitra, D., Byun, J., Sliskovic, I., Abdulhamid, I., Saed, G. M., et al. (2010). Potent
503 antioxidative activity of lycopene: a potential role in scavenging hypochlorous acid. *Free Radical*
504 *Biology and Medicine*, *49*, 205–213.
505 Riesz, P., Berdahl, D., & Christman, C. L. (1985). Free radical generation by ultrasound in aqueous
506 and nonaqueous solutions. *Environmental Health Perspectives*, *64*, 233.
507 Rivera, S. M., & Canela-Garayoa, R. (2012). Analytical tools for the analysis of carotenoids in diverse
508 materials. *Journal of Chromatography A*, *1224*, 1–10.
509 Rivera, S. M., Christou, P., & Canela-Garayoa, R. (2014). Identification of carotenoids using mass
510 spectrometry. *Mass Spectrometry Reviews*, *33*, 353–372.
511 Rodriguez, E. B., & Rodriguez-Amaya, D. B. (2009). Lycopene Epoxides and Apo-lycopenals formed

by chemical reactions and autoxidation in model systems and processed foods. *Journal of Food Science*, *74*, C674–C682.

Satomi, Y. (2012). Fucoxanthin induces *GADD45A* expression and G1 arrest with SAPK/JNK activation in LNCap human prostate cancer cells. *Anticancer Research*, *32*, 807–813.

Sommerburg, O., Langhans, C. D., Arnhold, J., Leichsenring, M., Salerno, C., Crifò, C., et al. (2003). β-carotene cleavage products after oxidation mediated by hypochlorous acid-a model for neutrophil-derived degradation. *Free Radical Biology and Medicine*, *35*, 1480–1490.

Sugawara, T., Matsubara, K., Akagi, R., Mori, M., & Hirata, T. (2006). Antiangiogenic activity of brown algae fucoxanthin and its deacetylated product, fucoxanthinol. *Journal of Agricultural and Food Chemistry*, *54*, 9805–9810.

Sugimura, R., Suda, M., Sho, A., Takahashi, T., Sashima, T., Abe, M., et al. (2012). Stability of fucoxanthin in dried *Undaria pinnatifida* (wakame) and baked products (scones) containing wakame powder. *Food Science and Technology Research*, *18*, 687–693.

Sun, Y., Ma, G., Ye, X., Kakuda, Y., & Meng, R. (2010). Stability of all-trans-β-carotene under ultrasound treatment in a model system: Effects of different factors, kinetics and newly formed compounds. *Ultrasonics Sonochemistry*, *17*, 654–661.

Sy, C., Dangles, O., Borel, P., & Caris-Veyrat, C. (2013). Iron-induced oxidation of (all-E)-β-carotene under model gastric conditions: kinetics, products, and mechanism. *Free Radical Biology and Medicine*, *63*, 195–206.

Takashima, M., Shichiri, M., Hagihara, Y., Yoshida, Y., & Niki, E. (2012). Capacity of fucoxanthin for scavenging peroxyl radicals and inhibition of lipid peroxidation in model systems. *Free Radical Research*, *46*, 1406–1412.

534 Van Boekel, M. A. (2008). Kinetic modeling of food quality: a critical review. *Comprehensive Reviews*
535 *in Food Science and Food Safety*, *7*, 144–158.
536 Van Breemen, R. B., Dong, L., & Pajkovic, N. D. (2012). Atmospheric pressure chemical ionization
537 tandem mass spectrometry of carotenoids. *International Journal of Mass Spectrometry*, *312*,
538 163–172.
539 Weesepoel, Y., Gruppen, H., de Bruijn, W., & Vincken, J. P. (2014). Analysis of palmitoyl
540 apo-astaxanthinals, apo-astaxanthinones, and their epoxides by UHPLC-PDA-ESI-MS. *Journal of*
541 *Agricultural and Food Chemistry*, *62*, 10254–10263.
542 Woodall, A. A., Lee, S. W. M., Weesie, R. J., Jackson, M. J., & Britton, G. (1997). Oxidation of
543 carotenoids by free radicals: relationship between structure and reactivity. *Biochimica et*
544 *Biophysica Acta (BBA)-General Subjects*, *1336*, 33–42.
545 Xia, S., Wang, K., Wan, L., Li, A., Hu, Q., & Zhang, C. (2013). Production, characterization, and
546 antioxidant activity of fucoxanthin from the marine diatom *Odontella aurita*. *Marine Drugs*, *11*,
547 2667–2681.
548 Ye, G., Lu, Q., Zhao, W., Du, D., Jin, L., & Liu, Y. (2014). Fucoxanthin induces apoptosis in human
549 cervical cancer cell line HeLa via PI3K/Akt pathway. *Tumor Biology*, *35*, 11261–11267.
550 Zhao, D., Kim, S. M., Pan, C. H., & Chung, D. (2014). Effects of heating, aerial exposure and
551 illumination on stability of fucoxanthin in canola oil. *Food Chemistry*, *145*, 505–513.
552 Zhang, Y. P., Fang, H., Xie, Q. L., Sun, J. P., Liu, R., Hong, Z., et al. (2014). Comparative evaluation
553 of the radical-scavenging activities of fucoxanthin and its stereoisomers. *Molecules*, *19*,
554 2100–2113.

555 **Figure Captions**

556 **Fig. 1.** Chemical structure of all-*trans* fucoxanthin.

557 **Fig. 2.** Spectral changes observed for reactions of fucoxanthin with (A) $KMnO_4$, (B)

558 OH^-, (C) $HClO/ClO^-$ and their kinetic analysis (D). *n*, kinetic order of reaction; R^2,

559 coefficient of determination.

560 **Fig. 3.** MS/MS spectra of (A) apo-11'-fucoxanthinal with *m*/*z* 293 (Peak 6) and (C)

561 apo-9'-fucoxanthinone with *m*/*z* 267 (Peak 16) produced by $KMnO_4$-accelerated

562 oxidation; MS/MS spectra of (B) apo-13-fucoxanthinone with *m*/*z* 307 (Peak 2)

563 produced by HCl/ClO^--accelerated oxidation.

564 **Fig. 4.** MS/MS spectra of (A) apo-13'-fucoxanthinone with *m*/*z* 333 (Peak 2), (B)

565 apo-15-fucoxanthinal with *m*/*z* 333 (Peak 3), (C) apo-15'-fucoxanthinal with *m*/*z* 359

566 (Peak 6) and (D) apo-14'-fucoxanthinal with *m*/*z* 359 (Peak 4) produced by

567 $KMnO_4$-accelerated oxidation.

568 **Fig. 5.** MS/MS spectra of (A) all-*trans*-apo-12-fucoxanthinal with *m*/*z* 425 (Peak 10),

569 (B) 9'-*cis*-apo-12-fucoxanthinal with *m*/*z* 425 (Peak 14), (C)

570 13'-*cis*-apo-12-fucoxanthinal with *m*/*z* 425 (Peak 15) produced by

571 $KMnO_4$-accelerated oxidation and their UV-vis spectra (D).

572

573

574 **Figures**

575 **Fig. 1**

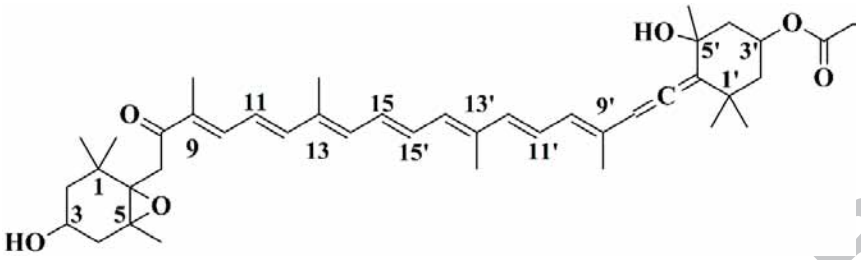

576

577 **Fig. 2**

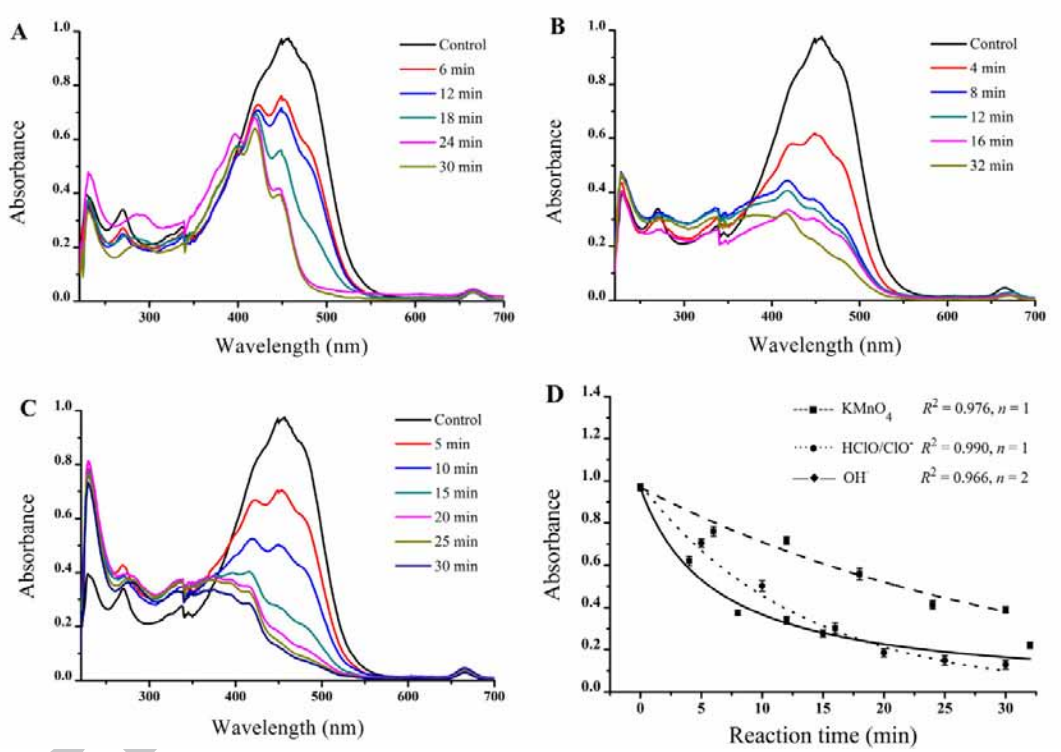

578

579

580

581

582

583

584

585

586

587 **Fig. 3**

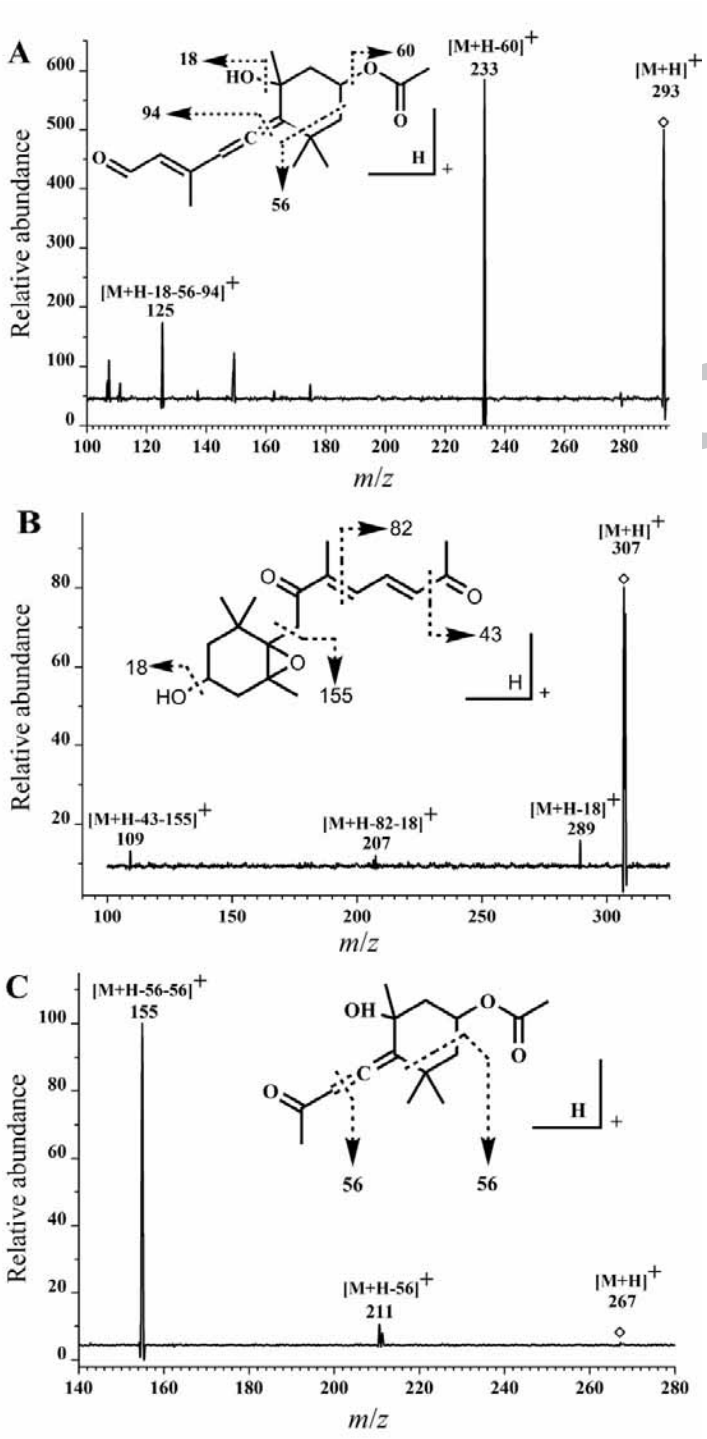

588

589

590

591

592 **Fig. 4**

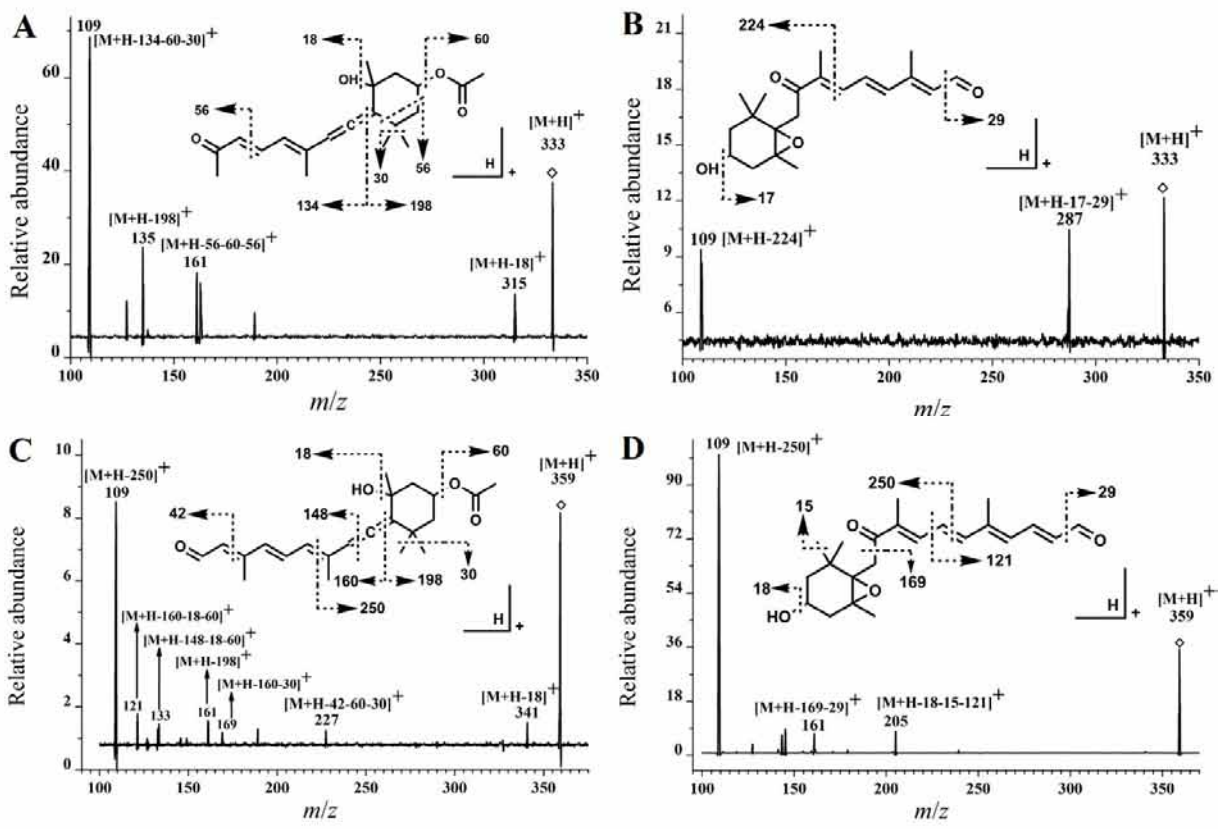

593

Fig. 5

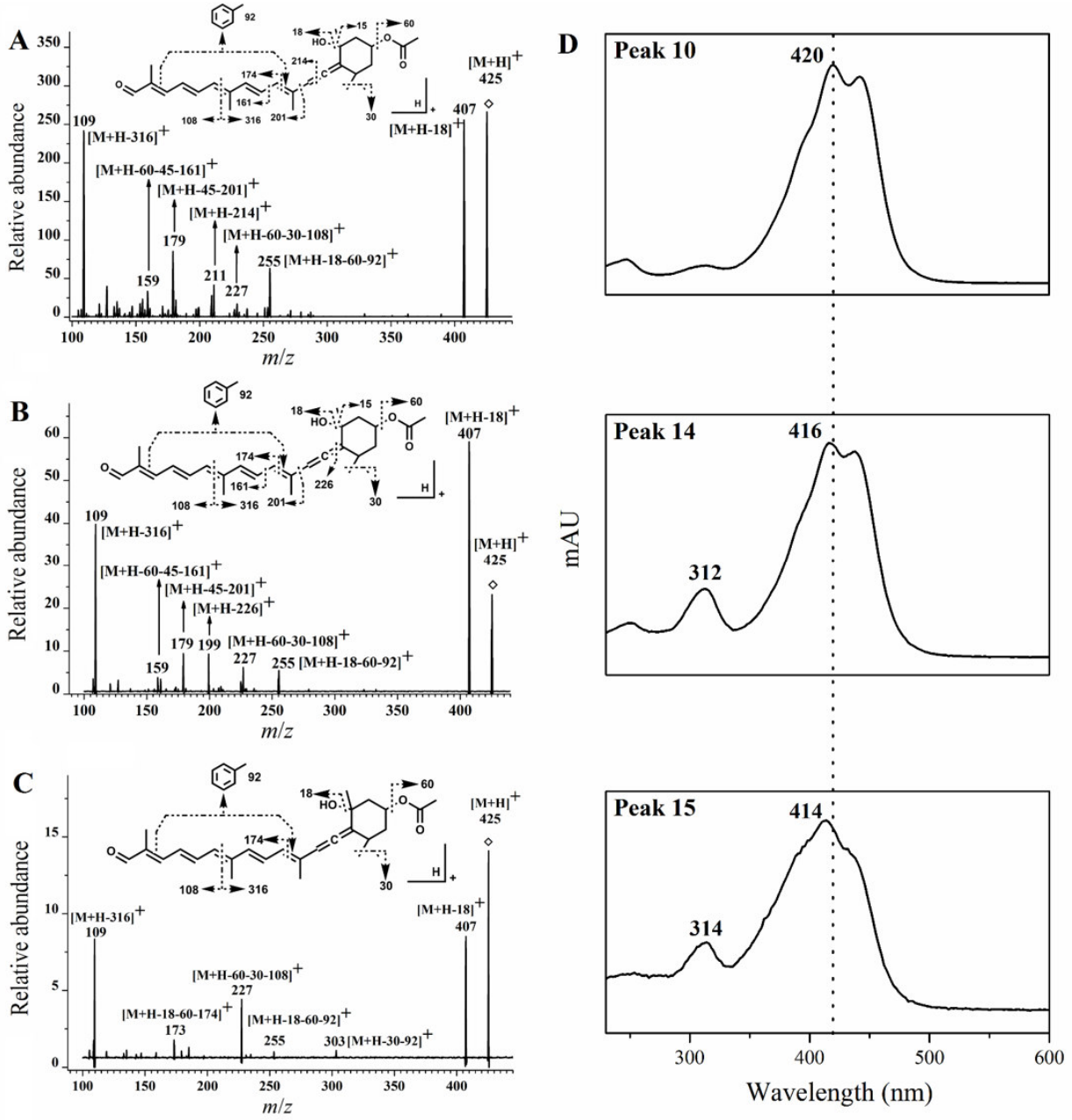

597 **Table 1.** Chromatographic and Mass Spectroscopic Properties of the Apo-fucoxanthins formed during Chemical Oxidation of Fucoxanthin

Identity	$[M + H]^+$ *m/z*	LC-APCI-MS/MS[c]	$KMnO_4$ reaction		$HClO/ClO^-$ reaction		OH^- reaction	
		m/z	Peak[a]	Rt[b] (min)	Peak[a]	Rt[b] (min)	Peak[a]	Rt[b] (min)
apo-13-fucoxanthinone	307	[307]: 289, 207, 109	ND[e]	ND[e]	2	3.140	2	3.133
apo-13'-fucoxanthinone	333	[333]: 315, 189, 163, 161, 135, 127, 109	2	3.307	3	3.313	3	3.307
apo-15-fucoxanthinal	333	[333]: 287, 109	3	3.460	4	3.445	4	3.440
apo-14'-fucoxanthinal	359	[359]: 205, 161, 145, 143, 109	4	3.560	5	3.560	5	3.547
apo-11'-fucoxanthinal	293	[293]: 233, 149, 125, 111, 107	5	3.727	6	3.725	6	3.720
apo-15'-fucoxanthinal	359	[359]: 341, 227, 189, 169, 161, 133, 121, 109	6	3.927	7	3.927	7	3.920
all-*trans*-apo-12'-fucoxanthinal	399	[399]: 381, 229, 201, 179, 173, 159, 153, 127, 109	9	4.627	11	4.620	11	4.607
all-*trans*-apo-12-fucoxanthinal	425	[425]: 407, 255, 227, 211, 179, 159, 127, 109	10	5.040	13	5.027	13	5.013
x-*cis*-apo-12'-fucoxanthinal[d]	399	[399]: 381, 229, 211, 201, 173, 133, 127, 109						
13,13'-*cis*-apo-12'-fucoxanthinal[d]	399	[399]: 381, 243, 173, 127, 109	11	5.253	14	5.267	15	5.247
13'-*cis*-apo-12'-fucoxanthinal[d]	399	[399]: 399, 229, 211, 201, 173, 127, 123, 109	12	5.540	15	5.547	16	5.540
9'-*cis*-apo-12-fucoxanthinal[d]	425	[425]: 407, 255, 227, 199, 179, 159, 109	14	6.047	16	6.060	17	6.033
13'-*cis*-apo-12-fucoxanthinal[d]	425	[425]: 407, 303, 255, 227, 173, 109	15	6.333	17	6.347	18	6.321
apo-9'-fucoxanthinone	267	[267]: 211, 155	16	6.880	18	6.898	19	6.920

598 [a]Peak assignments based on Fig. S3. [b]Retention time (Rt) refer to analytical runs on a XDB-C18 column. [c]Specific fragments of degradation products detected in the three
599 chemical reactions. [d]Five *cis*-apo-fuconxanthinals were temporarily identified according to Fig. 5, Fig. S5 and eluting order of *cis*-fucoxanthin. [e]ND, not detected.

600

601 **Highlights**

602 1. Chemical oxidation of fucoxanthin using $KMnO_4$, $HClO/ClO^-$ and OH^- displays a good fit to the first- or second-order kinetic models.

603 2. Apo-fucoxanthinones and apo-fucoxanthinals are detected as the predominant fucoxanthin cleavage products.

604 3. Three apo-fucoxanthinones and eleven apo-fucoxanthinals containing five *cis*-apo-fucoxanthinals are detected upon oxidation by $KMnO_4$,

605 $HClO/ClO^-$ and OH^-.

606

607